Clin Neuroradiol (2019) 29:741–749
https://doi.org/10.1007/s00062-018-0701-5

ORIGINAL ARTICLE

Iterative Algorithms Applied to Treated Intracranial Aneurysms

Aikaterini Fitsiori[1] · Steve Philippe Martin[2] · Alix Juillet De Saint Lager[2] · Joanna Gariani[1] · Karl-Olof Lovblad[1] · Xavier Montet[2] · Maria Isabel Vargas[1]

Received: 19 January 2018 / Accepted: 31 May 2018 / Published online: 19 June 2018

Abstract

Purpose To investigate the impact of iterative metal artifact reduction (iMAR) on artifacts related to neurosurgical clips or endovascular coils when combined to filtered back projection (FBP) or advanced modelled iterative reconstruction (ADMIRE).

Material and Methods In this study 21 unenhanced brain computed tomography (CT) examinations were reconstructed with FBP and level 2 of ADMIRE, both techniques with and without iMAR algorithm, resulting in 4 series per acquisition. Subjective assessment of artifact reduction was performed as a double-blinded evaluation with a 5-point-scale. Objective analysis was performed by comparing central tendencies and distributions of voxel densities. The central tendency was assessed as the mean voxel density in Hounsfield units. The distribution was assessed by evaluating the shape and asymmetry of the histograms of voxels densities with measures of kurtosis and skewness, respectively.

Results Inter-reader agreement was excellent (>0.8). FBP and ADMIRE without iMAR were scored 4 and with iMAR 5. Unusual artifacts were noted in all of the series reconstructed with iMAR, especially when combined with ADMIRE. Kurtosis revealed statistical differences for all reconstruction techniques ($p \leq 0.0007$) except for the association of FBP with iMAR ($p = 0.2211$) for the coiling population and skewness demonstrated no statistical difference in any population ($p \geq 0.0558$), confirming the subjective analysis results, except for the ADMIRE algorithm with or without iMAR ($p \leq 0.0342$) in the coiling population.

Conclusion iMAR led to the reduction in artifacts due to intracranial metallic devices. However, it created a new artifact in the form of a halo of photon-starvation, especially when combined with ADMIRE. The combination of FBP and iMAR seems more suitable, combining the beneficial metal artifact reduction without the emergence of a halo of photon starvation just around the point of interest.

Keywords Intracranial aneurysm · Computed tomography (CT) · Computer-assisted algorithms · Artifacts

Abbreviations

ADMIRE	Advanced modelled iterative reconstruction
CT	Computed tomography
CTDIvol	Computed tomography dose index volume
DLP	Dose-length product
FBP	Filtered back projection
HU	Hounsfield unit
iMAR	Iterative metal artifact reduction
IR	Iterative reconstruction
ROI	Region of interest
SD	Standard deviation

Part of this work has been presented in poster form at the Swiss Congress of Radiology, Bern, Switzerland, June 08–10, 2017. Please note that authors A. Fitsiori and S.P. Martin contribute equally and should be considered as co-first.

✉ Steve Philippe Martin
Steve.Martin@hcuge.ch

[1] Division of Neuroradiology, Department of Imaging and Medical Information Sciences, Geneva University Hospitals, Rue Gabrielle-Perret-Gentil 4, 1205 Geneva, Switzerland

[2] Division of Radiology, Department of Imaging and Medical Information Sciences, Geneva University Hospitals, Rue Gabrielle-Perret-Gentil 4, 1205 Geneva, Switzerland

Key Points

- Coils and clips constitute the modern treatment of intracranial aneurysms
- Metal artifacts due to coils and clips compromise follow-up image quality

- CT (computed tomography) manufacturers have developed several algorithms in order to reduce these artifacts
- iMAR (iterative metal artifact reduction) reduces the artifacts due to metal devices and raises the diagnostic confidence of the adjacent cerebral parenchyma

Introduction

Endovascular coiling and neurosurgical clipping are the recommended therapeutic options for intracranial aneurysms, depending on the particular characteristics of the aneurysm (form, size, location, accessibility), patient characteristics (age, comorbidities) and operator skills [1–5]. A combination of microsurgical and endovascular techniques is sometimes required in complex aneurysms [6].

Immediate posttreatment follow-up is necessary to evaluate possible complications, such as hemorrhage, stroke and edema. The appropriate imaging method remains a challenge because of image distortion related to artifacts produced by metal implants (coils and clips). In computed tomography (CT) the degradation of image quality is related to photon starvation and beam hardening artifacts, which encumber the study of brain parenchyma in the proximity of the metal device.

The first attempt to reduce metal artifacts in CT was published as early as 1981 by Glover and Pelc [7], followed by the studies of Kalender et al. in 1987 [8] and Klotz et al. in 1990 [9], whilst the first metal artifact reduction (MAR) algorithm was proposed by Prell et al. in 2010 [10] for use in interventional flat detector CT. This algorithm uses the replacement of underexposed pixels in proximity to the metal implant and interpolation of surrogate attenuation values for the original metal in the raw projection data domain. Since then, several algorithms have been proposed by CT manufacturers and different techniques reported by researchers [10–15], using different types of segmentation and interpolation on CT imaging. It is now widely accepted that the application of these metal artifact algorithms improves image quality [16, 17].

The primary outcome of our study was to objectively and subjectively assess the impact of iterative metal artifact reduction (iMAR), an algorithm specially designed by Siemens (Forchheim, Germany) to reduce metal artifacts, when combined with filtered back projection (FBP). It can also be combined with advance modelled iterative reconstruction (ADMIRE) on metal artifact reduction due to intracranial devices after treatment of aneurysms: ADMIRE is the third and latest generation of iterative reconstruction (IR) from Siemens. The secondary outcome was to objectively and subjectively evaluate the presence of unusual artifacts.

Material and Methods

The local ethics committee on research involving humans approved this retrospective study and waived the need for written consent (CCER2016-00111).

Patients

The study sample consisted of 21 computed tomography (CT) scans in a total of 18 patients sent to our department for follow-up after intracranial aneurysm treatment (12 treated by coiling and 9 by clipping), during a period of 10 months (from 26 April 2016 to 27 February 2017). The characteristics of the study sample are summarized in Table 1. All consecutive patients with intracranial coils or clips who underwent brain CT on our SOMATOM Definition Flash unit (Siemens Healthcare, Forchheim, Germany) were included. The exclusion criteria were the following: patients under 18 years of age and patients with other metallic devices in the field of acquisition, such as rigid neck braces, cochlear implants, deep brain stimulation electrodes, ventriculoperitoneal bypass valves or cranioplasty metallic devices.

Computed Tomography Acquisition, Reconstruction Parameters and Radiation Dose

Unenhanced brain CT examinations were performed as a single acquisition. The following acquisition parameters were used: collimation $64 \times 2 \times 0.6$ mm, pitch 0.6, rotation time 0.28 s, tube voltage 100 kV with CARE kV providing automated tube voltage adjustment, tube current 120 mAs ref. with CARE Dose4D providing automated tube current adjustment.

All 21 CT acquisitions were reconstructed with FBP and with level 2 of ADMIRE, both techniques with and without iMAR, resulting in 4 series per single patient acquisition (FBP alone, ADMIRE alone, FBP combined with iMAR and ADMIRE combined with iMAR). The following reconstruction parameters were used: slice thickness–interval 3–3 mm, kernel H/J40s and ADMIRE, the third generation of IR from Siemens, offers 5 levels of strength: for our study we used the same level of IR as we routinely use in our clinical practice, i.e. level 2. Dose-length product (DLP) and computed tomography dose index volume (CTDIvol) were provided by the manufacturer on the basis of a well-calibrated CT with a 16 cm phantom.

Image Analysis

Objective analysis was performed by comparing central tendency and distribution of voxel density. Data were obtained by carefully placing 2 standardized circular regions of inter-

Table 1 Characteristics of the study sample

	Endovascular coil	Neurosurgical clip
Number of CT examinations	12	9
Mean age [range] (years)	54 [27–70]	57 [30–74]
M/F ratio	1/2	2/1
Material	Platinum ($n=4$) Stainless steel ($n=3$) Both types ($n=5$)	Titanium ($n=9$)
Mean size [range] (long axis in mm)	12 [5–25]	19 [15–24]
Aneurysm localization (R = right; L = left)		
CA	2 (R); 1 (L)	1 (R)
OA	1 (R)	0
ACOA	4	5
ACHA	1 (R)	0
MCA	0	1 (R); 1 (L)
PCOA	1 (R); 1 (L)	2 (L)
PICA	2 (L)	0

CA carotid artery, *OA* ophthalmic artery, *ACOA* anterior communicating artery, *ACHA* anterior choroidal artery, *MCA* middle cerebral artery, *PCOA* posterior communicating artery, *PICA* posterior inferior cerebellar artery

est (ROI) measuring 5 cm^2 for each of the four reconstructed datasets. Fig. 1 demonstrates an example of ROI placement. The first ROI was positioned in the brain parenchyma in close proximity to the metal implant on the slice showing the most artifacts, without covering the metal implant. The second ROI, serving as unaltered control values, was positioned in the brain parenchyma on a distant slice of the metal implant showing no artifacts. The central tendency was assessed as the mean voxel density in Hounsfield units (HU). The distribution was assessed by evaluating the shape and the asymmetry of voxel density histograms with the measures of kurtosis and skewness, respectively.

Subjective analysis was performed as a double-blinded randomized visual assessment of all the reconstructed datasets by two board-certified neuroradiologists with 5 and 15 years of experience in imaging (A.F and M.I.V., respectively) within a period of 2 months. All images were evaluated on a standard brain window setting (window width = 100, window level = 50). Artifact presence was assessed on a 5-point Likert scale (1: artifacts severely altering diagnostic confidence [<50%] in all 4 quarters of the slice, 2: artifacts severely altering diagnostic confidence [<50%] in 3 quarters of the slice, 3: artifacts severely altering diagnostic confidence [<50%] in 2 quarters of the slice, 4: artifacts severely altering diagnostic confidence [<50%] in 1 quarter of the slice, 5: artifacts severely altering diagnostic confidence [<50%] only localized around the metal device). The readers were instructed to record any new or unusual artifacts. Re-sizing and level windowing were allowed.

Statistical Analysis

Study sample was evaluated as 2 separate populations according to the approach of treatment, either coiling or clipping. Each population was then divided in 4 matched groups according to the 4 combinations of reconstruction techniques (FBP alone, ADMIRE alone, FBP combined with iMAR and ADMIRE combined with iMAR). For the objective analysis mean densities in HU, kurtosis and skewness were compared with a P value <0.05 considered statistically significant. These results are given as means and standard deviation. These variables did not pass the D'Agostino and Pearson normality test with an alpha value equal to 0.05 and were analyzed with a post hoc pairwise comparison by Friedman test with Dunn's multiple comparisons test. For the subjective analysis the interreader agreement was measured by Cohen's kappa coefficient. The results are given as medians.

Results

Radiation Dose

The dose delivered (mean ± SD) was a DLP 1194 ± 308 mGy/cm and a CTDIvol 63 ± 15 mGy.

Image Analysis

Mean densities, kurtosis and skewness obtained from the 4 different reconstruction datasets for each acquisition are summarized in Table 2 for the endovascular approach and in Table 3 for the neurosurgical approach.

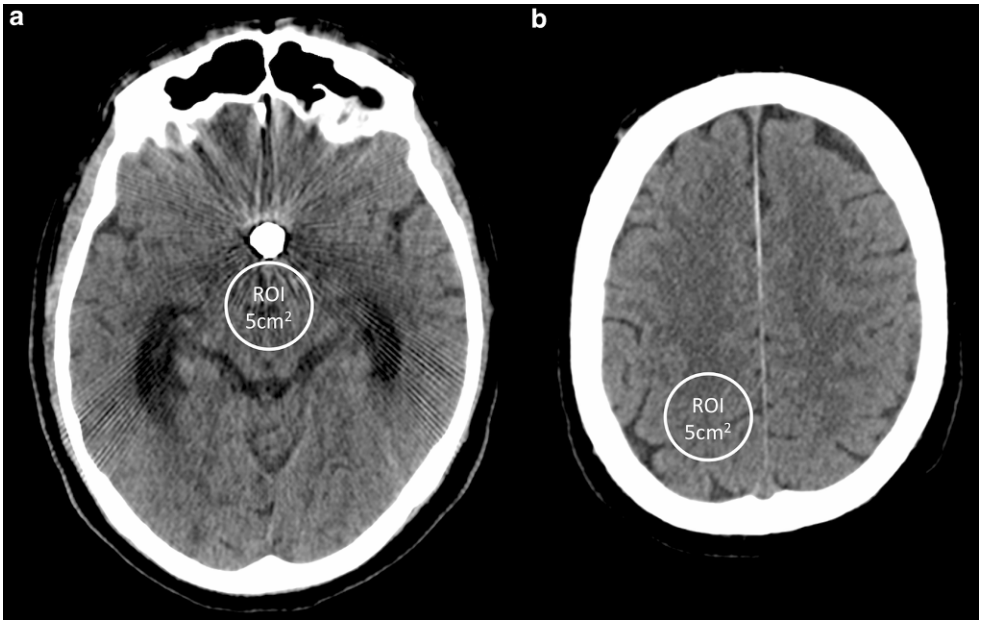

Fig. 1 Axial brain unenhanced CT images illustrating how the ROI were placed in the close proximity of metallic artifact due to a coiled aneurysm of the anterior communicating artery (**a**) and at a distant slice showing no artifact (**b**)

The central tendency was evaluated by comparing the mean densities of each single group with the mean densities of the group ADMIRE distant ROI as a control. The latter group was an obvious choice because it was free of metal artifacts and the reconstruction technique was the one we use in clinical daily practice. Similar central tendency in the 2 populations (coils and clips) was confirmed as the analysis of the mean densities revealed no statistical differences between any reconstructions (all p-values ≥0.0685 for the endovascular approach and $p \geq 0.7131$ for the neurosurgical approach).

Kurtosis and skewness were evaluated by comparing the means of the values close to the metal implant with the means of the values distant to the metal implant from a single reconstruction technique. In the coiling population, kurtosis revealed statistical differences for all reconstruction techniques ($p \leq 0.0007$) except for the association of the classical algorithm with specific metal artifact reduction algorithm (FBP with iMAR; $p = 0.2211$). On the contrary, in the clipping population, kurtosis showed no statistical differences for all reconstruction techniques except for the third generation of IR algorithm without iMAR (ADMIRE alone; p-value ranging from 0.1371 to >0.9999 and $p < 0.0001$, respectively). Skewness demonstrated no statistical differences in any populations (p-value ranging from 0.0558 to >0.9999), confirming the results of the analysis of the mean densities for the central tendency, except for the third generation of IR algorithm with iMAR ($p = 0.0071$). On the other hand, when evaluating skewness of the ROIs close to the metal implant by comparing the means of all groups with the mean of the group that showed no differences with the distant ROI, i.e. FBP with iMAR as a control group, the third generation IR algorithm with or without iMAR was found to be significantly different with the most negative value for the association of ADMIRE and iMAR (-1.77 ± 1.89, $p = 0.0133$).

For subjective analysis, the interreader agreement was excellent (=0.806). The FBP and ADMIRE without iMAR were scored 4 and with iMAR were scored 5. An unusual artifact in the form of a hypoattenuation halo around the metal device was noticed in all series reconstructed with iMAR; this artifact was particularly obvious when combined with ADMIRE.

Discussion

In this study we compared different types and generations of reconstruction algorithms to investigate if there was a significant reduction of metal artifacts after treatment of intracranial aneurysms. We believe that the efficient reduction of metal artifacts would allow an improvement in diagnostic confidence for the evaluation of structures adjacent to metal devices including post-treatment complications, such as hemorrhage, ischemia or edema. We deliberately chose not to assess enhanced brain CT or CT angiography, but only to assess unenhanced brain CT. The enhanced CT acquisitions are more prone to differences in contrast media uptake due to delay of contrast media injection [18] or upstream stenosis [19] making any rigorous quantitative comparisons impossible.

Our study objectively revealed that the application of specific metal artifact reduction techniques dramatically reduced image distortion around the metal devices

Table 2 Statistical results of quantitative assessment of artifacts due to endovascular coils

Mean density in HU	Mean	SD	*p*-value [a]	Summary
ADMIRE control	35.58	4.39	–	–
FBP coil	28.63	42.39	0.5608	ns
FBP control	32.53	9.76	>0.9999	ns
FBP + iMAR coil	33.86	11.54	>0.9999	ns
FBP + iMAR control	35.60	4.40	>0.9999	ns
ADMIRE coil	26.11	43.65	0.0685	ns
ADMIRE + iMAR coil	31.21	12.60	0.5608	ns
ADMIRE + iMAR control	35.64	4.39	>0.9999	ns
Kurtosis	Mean	SD	*p* value [a]	Summary
FBP coil	12.79	9.25	<0.0001	****
FBP control	0.17	0.50		
FBP + iMAR coil	3.63	4.94	0.2211	ns
FBP + iMAR control	0.18	0.43		
ADMIRE coil	12.74	9.71	<0.0001	****
ADMIRE control	0.25	0.70		
ADMIRE + iMAR coil	13.35	15.90	0.0007	***
ADMIRE + iMAR control	0.26	0.63		
Skewness intraRECON	Mean	SD	*p* value [a]	Summary
FBP coil	–0.98	2.06	>0.9999	ns
FBP control	–0.14	0.37		
FBP + iMAR coil	–0.38	0.86	>0.9999	ns
FBP + iMAR control	–0.15	0.34		
ADMIRE coil	–1.42	1.99	0.0558	ns
ADMIRE control	–0.13	0.44		
ADMIRE + iMAR coil	–1.77	1.89	0.0071	**
ADMIRE + iMAR control	–0.14	0.41		
Skewness interRECON	Mean	SD	*p* value [a]	Summary
FBP + iMAR coil	–0.38	0.86	–	–
FBP coil	–0.98	2.06	>0.9999	ns
ADMIRE coil	–1.42	1.99	0.0342	*
ADMIRE + iMAR coil	–1.77	1.89	0.0133	*

intraRECON means within the same reconstruction method
interRECON means between the different reconstruction method
ADMIRE advanced modelled iterative reconstruction, *iMAR* iterative metal artifact reduction, *FBP* filtered back projection, *HU* Hounsfield unit, *SD* standard deviation
ns > 0.05; * ≤ 0.05; ** ≤ 0.01; *** ≤ 0.001; **** < 0.0001
[a] post hoc pairwise comparison by Friedman test with Dunn's multiple comparisons test

(coils or clips) and thus improved the evaluation of brain parenchyma in areas where this was not previously possible because of excessive image noise. This observation was already apparent during the visual assessment of all reconstructed datasets by two participating neuroradiologists, as shown in Figs. 2 and 3 for the coiling and clipping population, respectively. They evaluated the influence of the artifact, with a score of 5 (best diagnostic confidence) for the iMAR with FBP or ADMIRE algorithms compared to a score of 4 for FBP or ADMIRE alone.

Moreover, objective analysis confirmed the results of our visual evaluation by revealing statistical differences in kurtosis (as shown in histograms on Figs. 4 and 5 for the coiling and the clipping population, respectively), in the coiling population, for all reconstruction techniques except for the association of FBP with iMAR ($p \leq 0.0007$ and $p = 0.2211$, respectively). This finding shows that the association of FBP and iMAR reconstruction algorithms can efficiently correct the distortion of the HU distribution (and consequently of the image) produced from the excessively high values in density of metal implants, as well as the underexposed values due to photon starvation phenomenon or beam hardening. This finding was not confirmed for the clipping population, for which statistical analysis did not reveal any significant differences. A possible explanation for this finding is that the differences in the texture and shape of coils

Table 3 Statistical results of quantitative assessment of artifacts due to neurosurgical clips

Mean density in HU	Mean	SD	*p*-value [a]	Summary
ADMIRE control	34.78	1.79	–	–
FBP clip	35.06	6.28	0.7131	ns
FBP control	34.66	1.77	>0.9999	ns
FBP + iMAR clip	35.03	6.47	>0.9999	ns
FBP + iMAR control	34.80	1.72	>0.9999	ns
ADMIRE clip	35.38	6.81	>0.9999	ns
ADMIRE + iMAR clip	35.51	6.43	>0.9999	ns
ADMIRE + iMAR control	34.96	1.73	>0.9999	ns
Kurtosis	Mean	SD	*p* value [a]	Summary
FBP clip	1.23	2.43	0.1371	ns
FBP control	0.03	0.49		
FBP + iMAR clip	0.19	0.53	>0.9999	ns
FBP + iMAR control	0.04	0.42		
ADMIRE clip	1.64	3.11	<0.0001	****
ADMIRE control	0.12	0.77		
ADMIRE + iMAR clip	0.35	0.77	>0.9999	ns
ADMIRE + iMAR control	0.13	0.70		
Skewness intraRECON	Mean	SD	*p* value [a]	Summary
FBP clip	–0.06	0.62	>0.9999	ns
FBP control	–0.20	0.24		
FBP + iMAR clip	0.01	0.36	0.1215	ns
FBP + iMAR control	–0.18	0.20		
ADMIRE clip	–0.10	0.75	>0.9999	ns
ADMIRE control	–0.23	0.31		
ADMIRE + iMAR clip	–0.04	0.45	>0.9999	ns
ADMIRE + iMAR control	–0.22	0.28		
Skewness interRECON	Mean	SD	*p* value [a]	Summary
FBP + iMAR clip	0.01	0.36	–	–
FBP clip	–0.06	0.62	0.5127	ns
ADMIRE clip	–0.10	0.75	0.3621	ns
ADMIRE + iMAR clip	–0.04	0.45	>0.9999	ns

intraRECON means within the same reconstruction method
interRECON means between the different reconstruction method
ADMIRE advanced modelled iterative reconstruction, *iMAR* iterative metal artifact reduction, *FBP* filtered back projection, *HU* Hounsfield unit, *SD* standard deviation
ns > 0.05; * ≤ 0.05; ** ≤ 0.01; *** ≤ 0.001; **** < 0.0001
[a] post hoc pairwise comparison by Friedman test with Dunn's multiple comparisons test

and clips (the coils usually produce more artifacts inherent to their texture and the coils usually produce round-shaped artifacts in comparison to more prominent artifacts in the long axis of asymmetrical devices such as clips), as well as the fact that coils are of various sizes depending on the aneurysm, while clips are less variable in size. As a result, the impact of the clips on the image quality is less important than the impact of the coils and therefore the improvement of image quality with the use of the reconstruction algorithms was not evident in our study for this group of patients.

The findings of our study are also consistent with those reported in previous studies [10–15], while other researchers have proposed different techniques to improve their diagnostic performance, such as monochromatic imaging [20, 21] or a head tilt technique [22], with some interesting results. The novelty of our study compared to previous ones lies on the use of both subjective and objective analysis of the different reconstructions techniques not only comparing the different techniques with a control but also among them. To our knowledge, this is the first time a complete assessment and comparison of different reconstruction techniques providing confirmation of the advantage of using these artifact-reducing techniques, with both visual and statistical quantitative analysis has been performed.

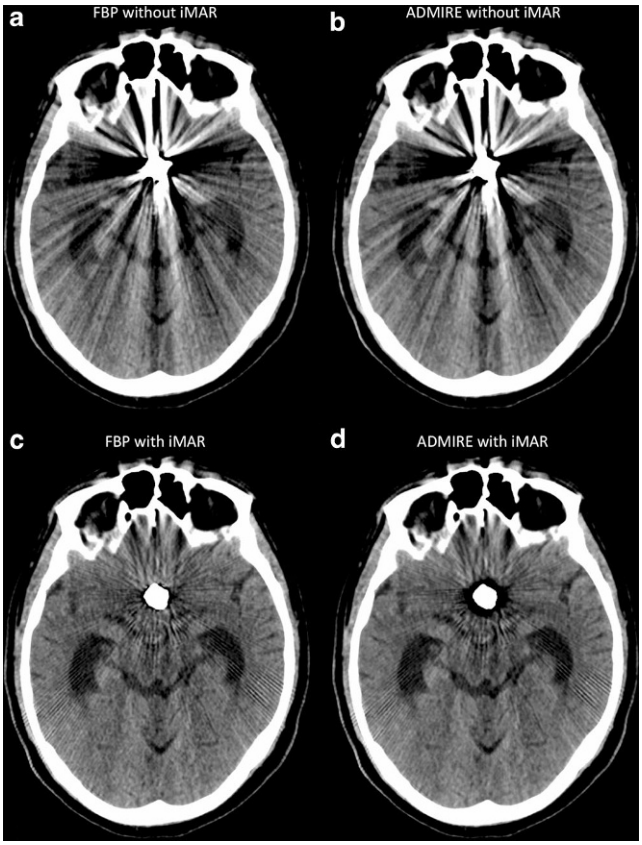

Fig. 2 Axial brain unenhanced CT images illustrating the 4 combinations of reconstruction from a single acquisition at the level of metallic artifact due to a coiled aneurysm of the anterior communicating artery. **a** and **b** show important beam hardening and photon starvation artifacts severely altering diagnostic confidence. **c** and **d** show obvious reduction of beam hardening and photon starvation artifacts on the reconstruction associated with iMAR. Also note the presence of an unusual artifact as thin halo loss of signal surrounding the coil in the reconstruction associated with iMAR, particularly evident in combination with ADMIRE (**d**)

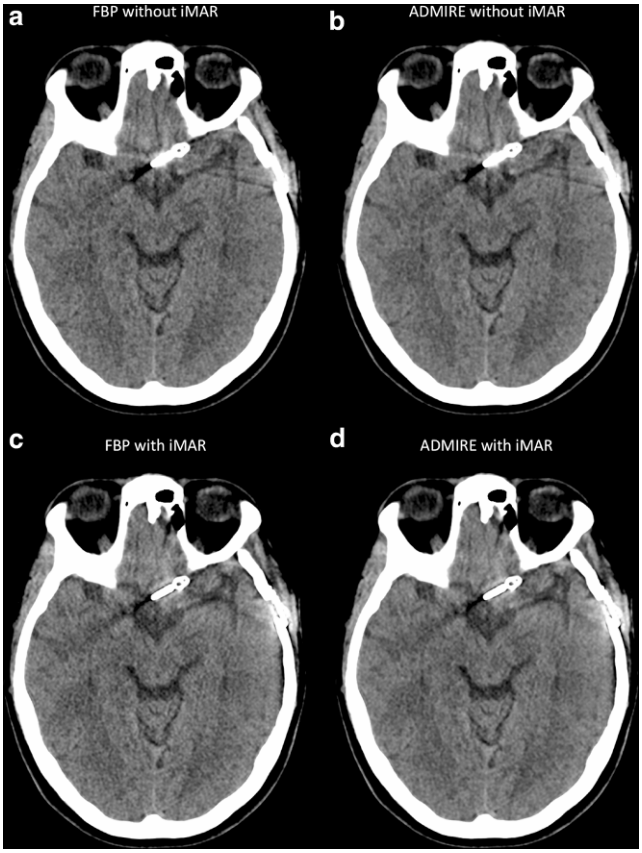

Fig. 3 Axial brain unenhanced CT images illustrating the 4 combinations of reconstruction from a single acquisition at the level of metallic artifact due to a clipped aneurysm of the anterior communicating artery. **a–d** show few beam hardening and photon starvation artifacts mildly altering diagnostic confidence

Another novel observation in our study was an unusual artifact, which was visually noticed most often in the series reconstructed with iMAR; this was particularly obvious when combined with the ADMIRE technique and to our knowledge it has not yet been reported in previous studies. This artifact was identified as a thin halo of signal loss surrounding the coil or the clip as illustrated in image d in Figs. 1 and 2. It is also interesting that there was clearly a more prominent artifact surrounding coils in comparison to clips. In the quantitative method, the third generation of IR algorithm with or without iMAR was significantly different with the most negative values for the association of ADMIRE and iMAR, when comparing the mean density of the ROI close to the metal implant with the ROI of the group that presented no difference in ROI values proximal or distal to the metal implant (the FBI with iMAR group). This is consistent with the new artifact observed around the metal implant with the visual assessment, in particular in the ADMIRE with iMAR coiling group. There are also some new subtle artifacts, related to the reconstruction techniques that have already been reported by other researchers, such as the subtle streaks caused by implementation of the iMAR protocol [14], which are probably due to the replacement of image pixels of the original x-ray data. These artifacts do not generally compromise image quality as severely as the artifacts related to the coil or clip.

A limitation of our study were the differences in material, size, location and shape of the metal coils or clips used, which were not taken into account in our analysis, apart from the distinction between coils and clips.

Conclusion

The implementation of iMAR significantly reduces artifacts due to intracranial metal devices for the treatment

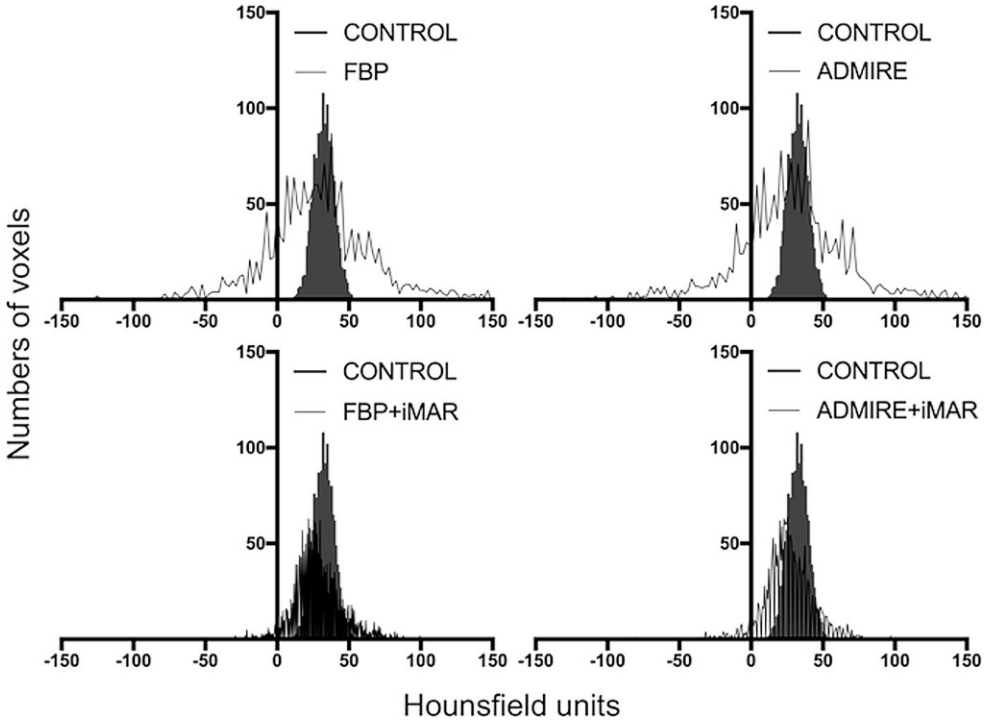

Fig. 4 Histograms of ROIs placed in the close proximity of an aneurysm treated by coil at the same level of the 4 different reconstructions from the same acquisition. The control ROI was placed on a slice distant to the artifact on the dataset reconstructed with ADMIRE 2 (reconstruction parameter clinically used in our daily practice)

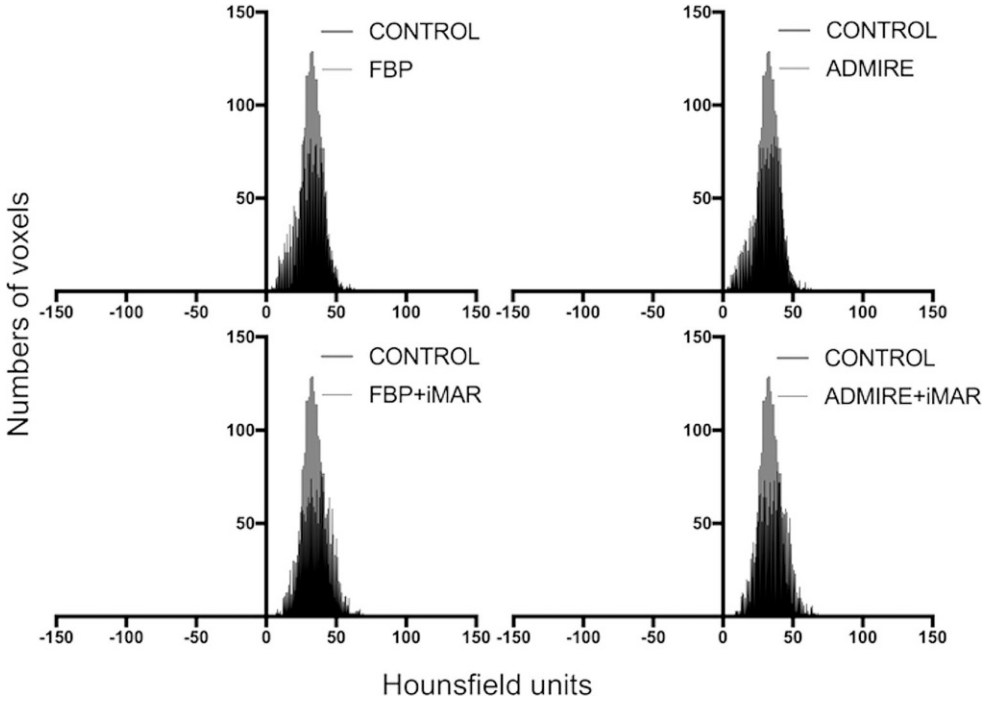

Fig. 5 Histograms of ROIs placed in the close proximity of an aneurysm treated by clip at the same level of the 4 different reconstructions from the same acquisition. The control ROI was placed on a slice distant to the artifact on the dataset reconstructed with ADMIRE 2 (reconstruction parameter clinically used in our daily practice)

of aneurysms and raises the diagnostic confidence for the evaluation of adjacent structures; however, iMAR was responsible for a novel artifact, a halo of photon starvation, which was particularly obvious in combination with ADMIRE. Even though we did not assess CT angiography for methodological reasons and in order to avoid bias, we believe that the combination of ADMIRE and iMAR should not be used for the evaluation of the neck of an aneurysm. The combination of FBP and iMAR seems more suitable, combining the beneficial metal artifact reduction without the emergence of a halo of photon starvation just around the point of interest.

Conflict of interest A. Fitsiori, S.P. Martin, A. Juillet De Saint Lager, J. Gariani, K.-O. Lovblad, X. Montet and M.I. Vargas declare that they have no competing interests.

References

1. Bederson JB, Awad IA, Wiebers DO, Piepgras D, Haley EC Jr., Brott T, Hademenos G, Chyatte D, Rosenwasser R, Caroselli C. Recommendations for the management of patients with unruptured intracranial aneurysms: a statement for healthcare professionals from the Stroke Council of the American Heart Association. Stroke. 2000;31:2742–50.
2. Lanzino G, Murad MH, d'Urso PI, Rabinstein AA. Coil embolization versus clipping for ruptured intracranial aneurysms: a meta-analysis of prospective controlled published studies. AJNR Am J Neuroradiol. 2013;34:1764–8.
3. Li H, Pan R, Wang H, Rong X, Yin Z, Milgrom DP, Shi X, Tang Y, Peng Y. Clipping versus coiling for ruptured intracranial aneurysms: a systematic review and meta-analysis. Stroke. 2013;44:29–37.
4. Molyneux A, Kerr R, Stratton I, Sandercock P, Clarke M, Shrimpton J, Holman R. International Subarachnoid Aneurysm Trial Collaborative, International Subarachnoid Aneurysm Trial (ISAT) of neurosurgical clipping versus endovascular coiling in 2143 patients with ruptured intracranial aneurysms: a randomised trial. Lancet. 2002;360(9342):1267–74.
5. Molyneux AJ, Kerr RS, Birks J, Ramzi N, Yarnold J, Sneade M, Rischmiller J, ISAT Collaborators. Risk of recurrent subarachnoid haemorrhage, death, or dependence and standardised mortality ratios after clipping or coiling of an intracranial aneurysm in the International Subarachnoid Aneurysm Trial (ISAT): long-term follow-up. Lancet Neurol. 2009;8:427–33.
6. Choudhri O, Mukerji N, Steinberg GK. Combined endovascular and microsurgical management of complex cerebral aneurysms. Front Neurol. 2013;4:108.
7. Glover GH, Pelc NJ. An algorithm for the reduction of metal clip artifacts in CT reconstructions. Med Phys. 1981;8:799–807.
8. Kalender WA, Hebel R, Ebersberger J. Reduction of CT artifacts caused by metallic implants. Radiology. 1987;164:576–7.
9. Klotz E, Kalender WA, Sokiransky R, Felsenberg D. Algorithms for the reduction of CT artifacts caused by metallic implants. Medical Imaging ′90, SPIE. 1990. p. 9.
10. Prell D, Kyriakou Y, Struffert T, Dörfler A, Kalender WA. Metal artifact reduction for clipping and coiling in interventional C-arm CT. AJNR Am J Neuroradiol. 2010;31:634–9.
11. Chintalapani G, Chinnadurai P, Srinivasan V, Chen SR, Shaltoni H, Morsi H, Mawad ME, Kan P. Evaluation of C-arm CT metal artifact reduction algorithm during intra-aneurysmal coil embolization: Assessment of brain parenchyma, stents and flow-diverters. Eur J Radiol. 2016;85:1312–21.
12. Pjontek R, Önenköprülü B, Scholz B, Kyriakou Y, Schubert GA, Nikoubashman O, Othman A, Wiesmann M, Brockmann MA. Metal artifact reduction for flat panel detector intravenous CT angiography in patients with intracranial metallic implants after endovascular and surgical treatment. J Neurointerv Surg. 2016;8:824–9.
13. Psychogios MN, Scholz B, Rohkohl C, Kyriakou Y, Mohr A, Schramm P, Wachter D, Wasser K, Knauth M. Impact of a new metal artefact reduction algorithm in the noninvasive follow-up of intracranial clips, coils, and stents with flat-panel angiographic CTA: initial results. Neuroradiology. 2013;55:813–8.
14. van der Bom IM, Hou SY, Puri AS, Spilberg G, Ruijters D, van de Haar P, Carelsen B, Vedantham S, Gounis MJ, Wakhloo AK. Reduction of coil mass artifacts in high-resolution flat detector conebeam CT of cerebral stent-assisted coiling. AJNR Am J Neuroradiol. 2013;34:2163–70.
15. Wuest W, May MS, Brand M, Bayerl N, Krauss A, Uder M, Lell M. Improved image quality in head and neck CT using a 3D iterative approach to reduce metal artifact. AJNR Am J Neuroradiol. 2015;36:1988–93.
16. Dolati P, Eichberg D, Wong JH, Goyal M. The utility of dual-energy computed tomographic angiography for the evaluation of brain aneurysms after surgical clipping: a prospective study. World Neurosurg. 2015;84:1362–71.
17. Fahrendorf DM, Goericke SL, Oezkan N, Breyer T, Hussain S, Sandalcioglu EI, Sure U, Forsting M, Gizewski ER. The value of dual-energy CTA for control of surgically clipped aneurysms. Eur Radiol. 2011;21:2193–201.
18. Shirasaka T, Hiwatashi A, Yamashita K, Kondo M, Hamasaki H, Shimomiya Y, Nakamura Y, Funama Y, Honda H. Optimal scan timing for artery-vein separation at whole-brain CT angiography using a 320-row MDCT volume scanner. Br J Radiol. 2017;90(1070):20160634.
19. Sasaki M, Kudo K, Ogasawara K, Fujiwara S. Tracer delay-insensitive algorithm can improve reliability of CT perfusion imaging for cerebrovascular steno-occlusive disease: comparison with quantitative single-photon emission CT. AJNR Am J Neuroradiol. 2009;30:188–93.
20. Jia Y, Zhang J, Fan J, Li C, Sun Y, Li D, Xiao X. Gemstone spectral imaging reduced artefacts from metal coils or clips after treatment of cerebral aneurysms: a retrospective study of 35 patients. Br J Radiol. 2015;88(1055):20150222.
21. Shinohara Y, Sakamoto M, Iwata N, Kishimoto J, Kuya K, Fujii S, Kaminou T, Watanabe T, Ogawa T. Usefulness of monochromatic imaging with metal artifact reduction software for computed tomography angiography after intracranial aneurysm coil embolization. Acta Radiol. 2014;55:1015–23.
22. Brown JH, Lustrin ES, Lev MH, Ogilvy CS, Taveras JM. Reduction of aneurysm clip artifacts on CT angiograms: a technical note. AJNR Am J Neuroradiol. 1999;20:694–6.